



## INTELLIGENT CONTROL TECHNIQUES FOR ENHANCING POWER TRANSFER CAPABILITY IN HVDC SYSTEMS: ADAPTIVE PI CONTROLLER TUNING WITH AI-BASED METHODS

**Mr. Brijesh Kumar**, MTech Scholar, Department of Electrical & Electronics Engineering, RKDF College of Engineering Bhopal (MP)

**Mr. Pramod Kumar Rathore**, Assistant Professor, Department of Electrical & Electronics Engineering, RKDF College of Engineering Bhopal (MP)

### ABSTRACT:

Alternating Current (AC) is the main driving force in industries and residential areas. However, for long transmission lines, AC transmission becomes more expensive and complicated compared to Direct Current (DC) due to frequency-related issues. HVDC (High Voltage Direct Current) technology has enabled efficient long-distance bulk power transfer and helps resolve challenges such as voltage stability and fault current reduction in AC networks. This thesis focuses on enhancing the power transfer capability of an HVDC transmission system by using intelligent control techniques. Specifically, it explores the adaptive tuning of a conventional PI controller with Artificial Intelligence (AI)-based methods such as fuzzy logic, neural networks (ANN), and adaptive neuro-fuzzy inference systems (ANFIS). These AI controllers are used to improve the dynamic performance of the HVDC system. A simulation model using MATLAB/SIMULINK with a 12-pulse thyristor converter and the CIGRE Benchmark Model 2 was developed to study system performance. Simulation results confirmed that AI-based controllers significantly improved the damping of post-fault oscillations and reduced the time to reach steady-state, with ANFIS achieving the best overall performance.

**Keywords:** HVDC Transmission; PI Controller; Artificial Intelligence; Fuzzy Logic; Neural Network (ANN); ANFIS Controller

### INTRODUCTION :

HVDC technology offers cost-effective, long-distance power transmission capabilities coupled with impedance power regulation. The appropriate design of HVDC controllers enhances the overall efficacy of the AC/DC system. Over the past 28 years, basic HVDC system models that connect DC linkages to robust AC systems have demonstrated inadequacy in developing a flexible modeling capability. The performance of subcomponents in weak systems and HVDC links, including rectifiers, inverters, mercury arc rectifiers, thyristors, IGBTs, IGCTs, standard PI controllers, and sophisticated controllers, is all affected [11].

The fluctuating system circumstances and saturation characteristics of transformers hindered the attainment of comprehensive control over HVDC systems. The non-linearity of harmonics produced by the HVDC system and filters rendered the system complex. The advancement of high voltage DC system studies for enhanced performance under varied situations to achieve optimal dynamic responses in practical power systems presents challenges in mathematical modeling without assumptions, due to their nonlinear and complicated nature [12].

Methods or approaches must be devised to mitigate the limitations of the systems based on mathematical models. The control technique should be straightforward in design for implementation, incorporating superior qualities such as:

- Wide operating range,
- Adapt to dynamic changes in system conditions and parameters,
- Operation for nonlinear and transient loads,
- Work without a detailed mathematical model.

These strategies should be effective even in the absence of a comprehensive mathematical model of the system. An ANN-based controller has supplanted the traditional PI controller on the rectifier side of the HVDC lines. Furthermore, the integration of artificial neural networks with fuzzy logic has demonstrated efficacy as a robust approach for managing highly nonlinear loads. ANN controllers

possess an edge over fuzzy logic controllers because to their capacity for learning and adaptability. However, controllers utilizing artificial neural networks (ANN) are impractical for highly uncertain systems, as they are incapable of processing data characterized by language factors. Consequently, an appropriate integration of these two methodologies into a singular system mitigates their respective shortcomings, and this system is referred to as ANFIS systems [13].

The necessity to build adaptive controllers, such as AI controllers, to improve the performance of high voltage DC systems, given their promising outcomes in power system control, was the primary impetus for this effort. This effort focuses on developing AI techniques for the HVDC system controller to enhance performance while ensuring adaptation to fluctuating operational conditions. The constant gains of PI controllers at the rectifier and inverter terminals are inadequate to manage the complexities of the HVDC system across a broad operational spectrum.

The drawbacks include prolonged recovery time and commutation failure when HVDC is linked to a poor AC system, resulting in system non-performance. Additionally, there are several concerns associated with the fixed PI Controller.

- Individuality to performance over a varied operating condition
- Recovery time
- Commutation failure under fault conditions when placed in weak AC systems.

One approach to circumvent this issue is to substitute the PI Controller with a new controller. This would entail significant expense. A further technique suggested in by the CIGRE working group is to incorporate the frequency of the AC system in the controller design, alongside the regulation of other parameters such as voltage and current. This technique is prone to instability under transient and dynamic circumstances [14].

An alternate proposed solution was the strengthening of the performance of the PI controller across a broad spectrum of operating conditions and faults. Artificial Intelligence techniques are proposed to supplant PI Controllers to enhance power system stability. Consequently, this research concentrates on developing AI methodologies for the tuning of conventional PI Controllers in HVDC systems, which will adapt to diverse operational conditions for improved stability and performance. The primary purpose of this research endeavor is:

- To develop fuzzy logic, ANN and ANFIS controllers for current control on rectifier and V and I control on inverter side.
- To compute the performance of HVDC system along the two sides of the line using the proposed AI techniques and conventional PI Controller.
- Evaluate the performance during faults of the controllers.

The HVDC system analyzed is the CIGRE Benchmark model, featuring twelve pulse converters rated at 100 MV, operating at 500 kV and 2 kA, connected to a weak AC system with a short-circuit ratio of 2.5 on both the rectifier and inverter sides [15]. The primary contributions of this paper are as follows:

- Creation of a MATLAB Simulink model for the CIGRE benchmark system and assessment of its performance under steady-state conditions.
- Comprehensive performance assessment of the CIGRE system under diverse fault situations at the rectifier/inverter terminals, including single-line-to-ground (SLG) fault, line-to-line-to-ground (LLG) fault, three-phase (LLL) fault, and direct current (DC) fault.
- Evaluation of the development and performance of Fuzzy Logic Controllers for the adaptive tuning of Proportional-Integral controllers at the rectifier and inverter terminals.
- Development and performance assessment of an ANN controller for the adaptive tuning of PI controllers at the rectifier and inverter terminals.
- Execution of ANFIS Controller.

## LITERATURE REVIEW :

**Junjie Hou; Guobing Song; Yanfang Fan [1]** A fault identification technique for protection and adaptive reclosing is presented for a hybrid multi-terminal HVDC system to enhance the dependability of fault isolation and reclosing. A fault identification approach is proposed by studying the "zero passing" characteristic of current at the local end during the converter capacitor discharge phase.

**Yi Lin; Yuchen Tang; Wei Wu; Cangbi Ding; Chenyi Zheng; Yi Tang [2]** Hybrid HVDC transmission is an efficient method for the long-distance transmission of offshore wind farms (OWFs). Reactive power compensation must be designated at the sending end of the offshore wind farm, potentially encompassing several offshore transformer stations and the rectifier station of the HVDC system.

**Sunita S. Biswal; Dipak Ranjan Swain; Shiba R. Paital; Pravat Kumar Rout [3]** This article emphasizes the essential elements of a multi-infeed voltage source converter (VSC)-based high voltage direct current (HVDC) system, including the modeling and simulation of a fractional order PI (FPI) controller. Owing to their fragmentary attributes, fractional-order PI (FPI) controllers exhibit greater durability than PI controllers in multi-infeed VSC HVDC (MiVDC) systems. The FPI parameters profoundly influence the controller's efficacy and require appropriate configuration.

**Guessabi Anwar; Gherbi Ahmed; Chebabhi Ali [4]** The contemporary utilization of power electronics devices for high voltage transmission significantly impacts power grid stability. This study examines the potential enhancement of dynamic stability through the regulation of voltage source converter-based high-voltage direct current systems (VSC-HVDC). The system voltages and currents are presented in the synchronous reference frame (dq-frame) to independently regulate active and reactive power.

**Bo Zhang; Xiong Du; Chengmao Du; Jingbo Zhao; Fangyuan Li [5]** The multi-terminal modular multilevel converter (MMC) for power transmission represents the prevailing trend in direct current (DC) transmission development. However, due to its rapid control and dynamic properties, it may interact with other inductive devices or the grid, resulting in stability difficulties. This paper elucidates the application of impedance analysis in the frequency domain for assessing system stability.

**Sihua Wang; Lijun Zhou; Tian Wang; Tianyu Chen; Yu Wang [6]** The multi-terminal high voltage direct current (MT-HVDC) grid has extensive potential applications in linking diverse energy sources, facilitating asynchronous interconnections of power grids, supplying electricity to remote loads, and other domains. The current pivotal technologies influencing the advancement of MT-HVDC transmission systems encompass prompt fault detection and localization within the DC line, as well as its speedy isolation.

**Tingwei Xu; Sheng Lin; Dalin Mu; Liping Zhao [7]** The current inverter station protection will malfunction during external faults. A defect area identification system utilizing wavelet energy ratio for inverter stations is suggested. This scheme analyzes the features of the existing fault component between the primary side of the converter transformer and the AC filter outlet, revealing significant distinctions between internal and external faults.

**Xiuyong Yu; Liye Xiao [8]** This study proposes a protection strategy for modular multilevel converter-based HVDC grids to satisfy the ultra-fast, selective, and reliable needs of DC fault protection. The protection scheme comprises main protection, directional pilot protection, and faulty pole identification.

**Ashutosh Kumar Tamrakar; Ebha Koley [9]** This work presents a protection strategy based on support vector machines (SVM) for a hybrid AC-HVDC transmission line integrated with a wind farm. The suggested technique can identify problems in both AC and HVDC lines. This technique commences with the acquisition of time-domain current and voltage signals at the relay point. The Discrete Fourier Transform is employed to estimate the fundamental components of current and voltage data, which are subsequently input into the SVM-based fault detection and classifier.

**Yingyu Liang; Yaotong Huo [10]** The multi-terminal direct current (MTDC) grid necessitates stringent standards for DC line protection, thereby requiring little transient information to swiftly and accurately ascertain the fault location. An enhanced Hausdorff distance technique is suggested to

address fake data by analyzing the waveform discrepancies between both sides of the protected transmission line during internal and external failures.

**ARTIFICIAL INTELLIGENT CONTROL OF HVDC TRANSMISSION SYSTEM:**

The use of an efficient and sophisticated current controller, developed utilizing AI methodologies such as fuzzy logic, neural networks, and neuro-fuzzy logic, enhances the performance of a high-voltage direct current transmission system. Figure 1 illustrates the block diagram of the HVDC system integrated with an AI controller.

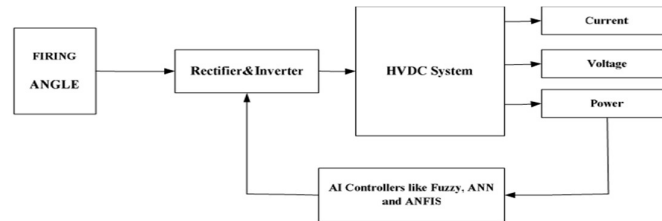


**Figure 1. Block diagram of the Proposed HVDC System**

**DESIGNS TO FUZZY LOGIC CONTROLLER (FLC):**

Fuzzy set theory use language values to denote imprecise concepts. The unpredictability of an event's occurrence is characterized as randomness, whereas the vagueness of the event is denoted as fuzziness. It is a straightforward expansion of a classical set, formally defined by assigning each potential individual element in a universal set a membership value ranging from -1 to 1 through membership functions. The FLC comprises four stages: Figure 2 illustrates the four stages.

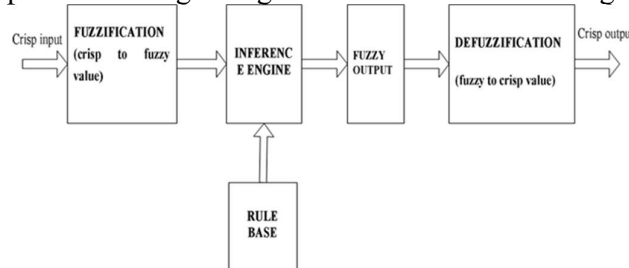


**Figure 2 Constitution diagram of fuzzy logic control system**

The performance parameters are aggregated in Tables 1 (rectifier) and 2 (inverter).

**Table 1 Performance Characteristics of Rectifiers with Fuzzy Logic Controller**

	Rise Time (Sec.)		Settling Time (Sec.)		%peak over shoot	
	PI	FLC	PI	FLC	PI	FLC
DC Fault	0.4573	0.2710	2.2780	1.8061	88.3956	72.3136
S-L-G Fault	0.8520	0.7048	1.9946	1.6903	71.5081	48.7094
L-L Fault	0.9243	0.7287	2.2162	1.8319	77.5264	60.6925
3-Phase Fault	0.9002	0.7252	2.0696	1.7850	82.9389	63.5516

**Table 2 Inverter performance characteristics with Fuzzy logic controller**

	Rise Time (Sec.)		Settling Time (Sec.)		%peak over shoot	
	PI	FLC	PI	FLC	PI	FLC
DC Fault	1.2095	0.9929	2.1656	1.7827	1.9452	1.7785
S-L-G Fault	1.0784	0.8855	2.0100	1.6709	2.1615	1.6684
L-L Fault	1.0972	1.0098	2.0202	1.8028	3.1464	2.4838
Three Phase Fault	1.0374	1.0285	1.9798	1.7606	2.2260	1.8627

Tables 1 and 2 demonstrate that both controllers enhance the performance of the HVDC system for rise time, settling time, peak, and percentage peak overshoot. The comparison of the two controllers indicates that the fuzzy logic controller demonstrates superior performance.

**ARTIFICIAL NEURAL NETWORK & ADAPTIVE NEURO-FUZZY INFERENCE SYSTEM (ANFIS) CONTROL OF HVDC TRANSMISSION SYSTEM:**

**ARCHITECTURE OF ARTIFICIAL NEURAL NETWORK FOR HVDC SYSTEM:**

Figure 3 illustrates the block diagram of the artificial neural network controller employed for the adaptive tuning of the PI Controller's gain.

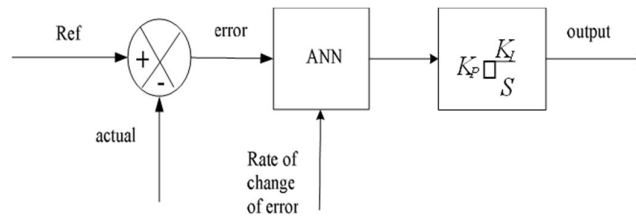


**Figure 1 Block diagram of ANN Controller**

**Table 3 Parameters of ANN controller**

Types of Neural Network considered	Feedforward Neural Network
Types of Learning Algorithm	Levenberg-Marquardt Algorithm
No of Hidden Layers	50
Value of Learning Rate	0.01
Activation Function (hidden)	tan sigmoid
Activation Function (output)	Linear
No of epochs used for training	1000
No of training Samples	10000

The flowchart for training of ANN is shown in Fig. 4.

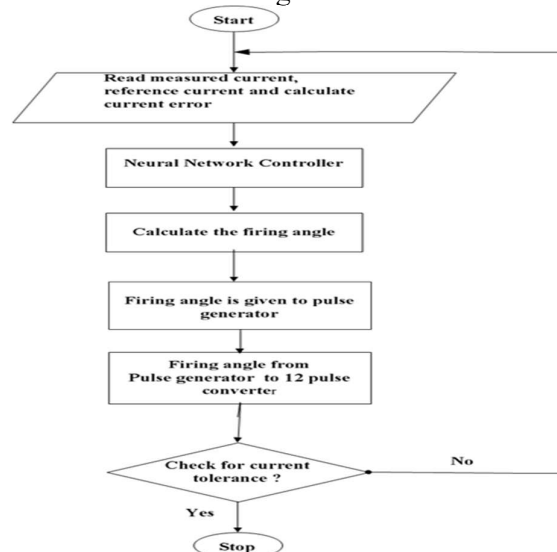


**Figure 4 Flowchart for training of ANN controller**

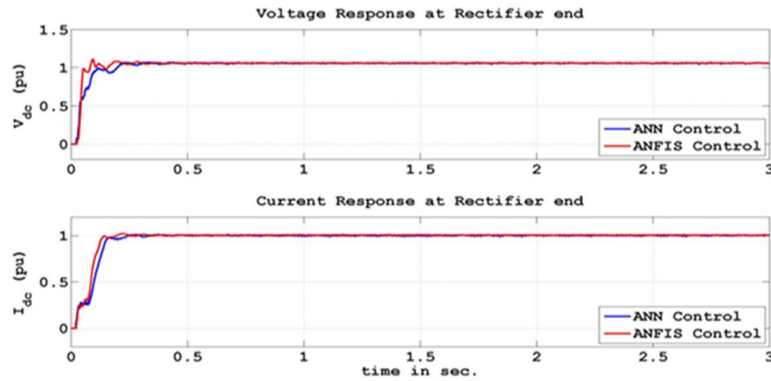
**SIMULATION RESULTS & DISCUSSION :**

A detailed HVDC system simulation model incorporating ANN and ANFIS controllers has been developed for both defect-free and faulty ANN scenarios. The ANN controller uses weight modification, while ANFIS uses a training approach. The system is tested under DC and AC faults, including single-line-to-ground, line-to-line, and three-phase faults. Comparative analysis shows

ANFIS outperforms PI, Fuzzy Logic, and ANN controllers. Simulation parameters are listed in Appendix 'A', and **Figures 5 to 22** present the stability analysis. Results are recorded at 3 seconds for both controllers across all fault conditions.

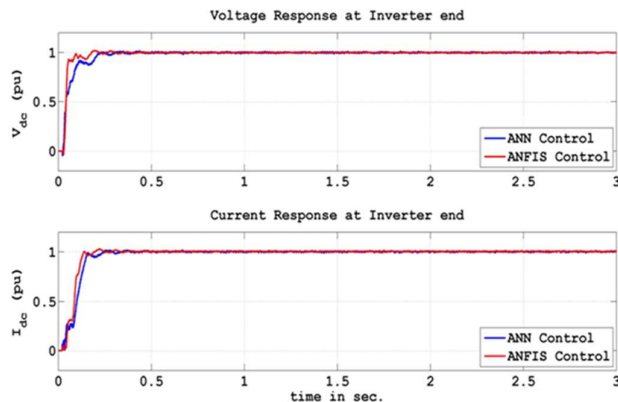
**WITHOUT FAULT :**

Figures 5, 6 and 7 illustrate the resultant waveforms at the rectifier and inverter terminals in the absence of defects, respectively.



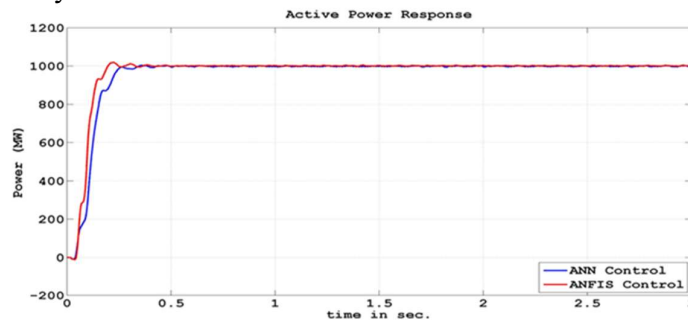
**Fig. 5 Voltage and Current Response of ANN and ANFIS Controller to DC side of Rectifier end**

Figure 5 shows that the ANFIS controller reaches the reference value of 1.0 pu at the rectifier end by 0.2 seconds, while the ANN controller does so at 0.3 seconds. This evaluates how long it takes for harmful transients to settle and the system to reach steady state.



**Fig. 6 Voltage and Current Response of ANN and ANFIS Controller to DC side of Inverter end**

Figure 6 presents the current and voltage waveforms of the ANN and ANFIS at the inverter terminal. While both perform well under faultless conditions, the ANFIS controller shows a slightly better ability to achieve a smooth steady state.

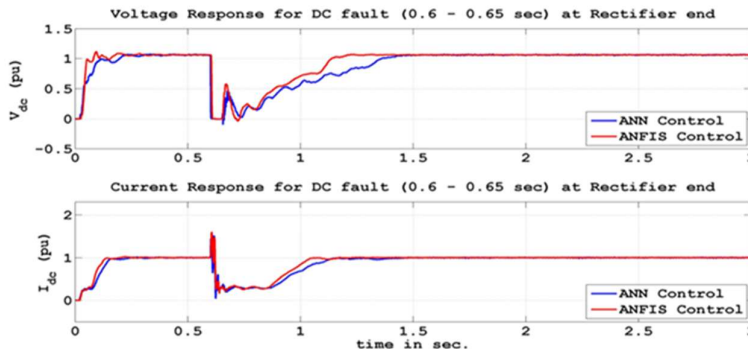


**Fig. 7 Active Power Response of ANN and ANFIS Controller**

Figure 7 shows the active power waveform, where the ANFIS controller delivers a smooth transient response, reaching steady state within 0.2 seconds.

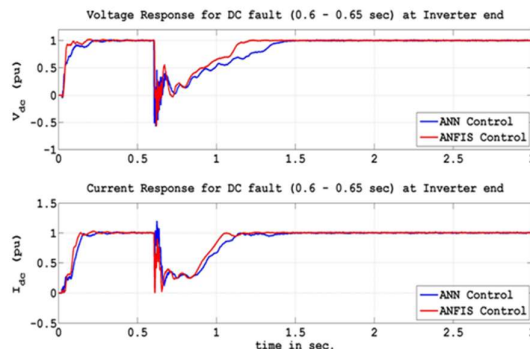
**DC FAULT:**

Figures 8, 9, and 11 display the current waveforms at the rectifier and inverter terminals, along with the active power of the ANN and ANFIS controllers under DC fault conditions. A steady state is reached at 0.5 seconds, after which a DC fault is introduced at the rectifier end at 0.6 seconds and cleared at 0.65 seconds.



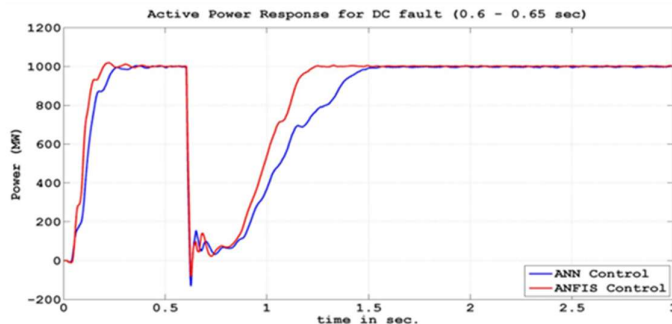
**Fig. 8 Voltage and Current Response of ANN and ANFIS Controller to DC fault at Rectifier end**

Figure 8 shows the voltage and current waveforms during a DC fault at the rectifier terminal. ANFIS displays fewer oscillations than ANN, with improved rise time (0.1462s), overshoot (52.11%), and settling time (1.1585s), compared to ANN's 0.1945s, 60.71%, and 1.4315s, respectively—highlighting ANFIS's superior performance.



**Fig. 9 Voltage and Current Response of ANN and ANFIS Controller to DC fault at Inverter end**

At 0.2 seconds, the system reaches steady state after initial transients. A DC fault is then applied at the inverter end at 0.6 seconds and cleared at 0.65 seconds. Figure 9 shows the current and voltage waveforms, where the ANN controller exhibits more oscillations, higher overshoot, and a longer settling time compared to the ANFIS controller.



**Fig. 10 Active power Response of ANN and ANFIS Controller to DC fault**

Figure 10 illustrates the active power response to a DC fault in an HVDC system, where the ANFIS controller shows a slight improvement over the ANN controller.

### Step Changes in Current Order (20%)

Figures 11, 12, and 13 illustrate the currents at the rectifier and inverter terminals, as well as the active power of the ANN and ANFIS controllers, in response to a 20% step change in current command.

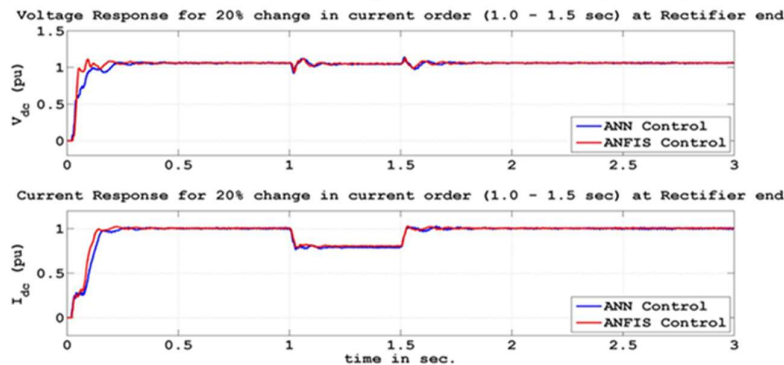


**Fig. 11 Voltage and Current Response of ANN and ANFIS Controller to 20% Step Change in current order at rectifier end**

A 20% step change in the current command on the rectifier side is initiated at 1 second, shifting the reference from 1.0 Pu to 0.8 Pu. The reference is then restored to 1.0 Pu at 1.5 seconds. The results are shown in Figure 11. The performance of both controllers shows no significant difference, as the fault severity is low.



**Fig. 12 Voltage and Current Response of ANN and ANFIS Controller to 20% Step Change at inverter end**

Figure 12 illustrates the current and voltage waveforms at the inverter terminal. During the 20% step change in the current command between 1 second and 1.5 seconds, the ANFIS controller shows fewer oscillations and reaches steady state more quickly than the ANN controller.

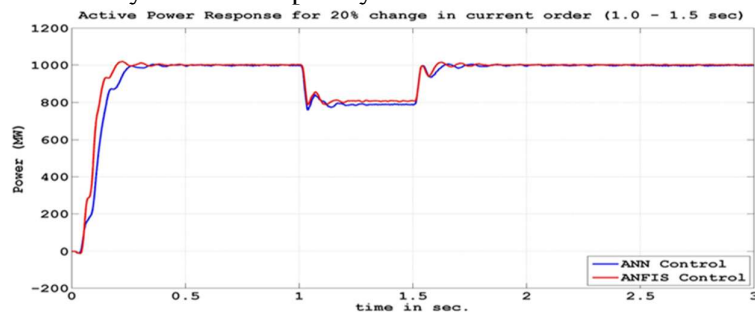
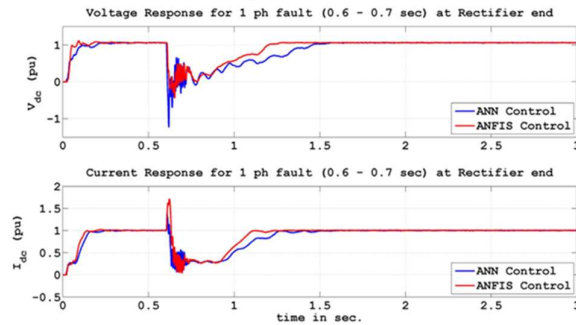


**Fig. 13 Voltage and Current Response of ANN and ANFIS controller to 20% step change**

Figure 13 illustrates the active power waveform. A 20% step change in the current command begins at 1 second, shifting the reference from 1.0 Pu to 0.8 Pu, and is restored to 1.0 Pu at 1.5 seconds. The responses of both controllers are closely aligned with no significant differences, although the ANFIS controller shows a more refined response and reaches steady state more smoothly than the ANN controller.

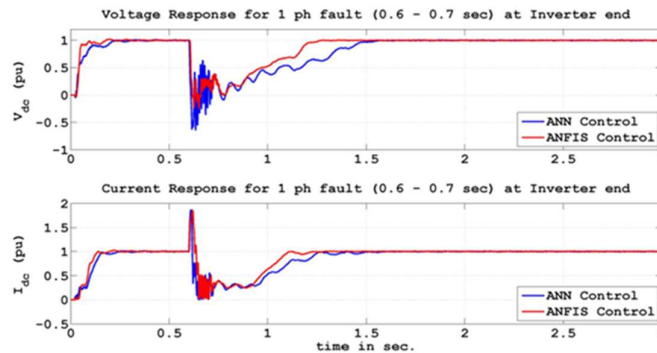
**SINGLE LINE TO GROUND FAULT :**

A single line-to-ground fault on phase A of the load side at the inverter terminal is analyzed to assess the performance of the rectifier and inverter using ANN and ANFIS controllers. The fault occurs at 0.6 seconds and is cleared at 0.7 seconds. Figures 14, 15, and 16 illustrate the current, voltage, and power waveforms related to the single line-to-ground fault.



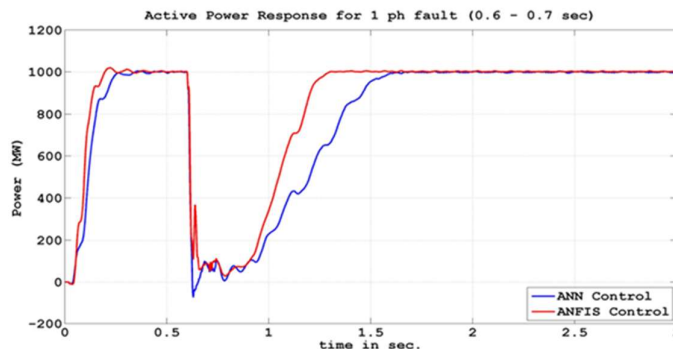
**Fig. 14 Voltage and Current Response of ANN and ANFIS controller to Single line to ground fault at rectifier end**

Figure 14 illustrates the current and voltage waveforms of the PI and fuzzy controllers during a single line-to-ground fault. The rise time for ANFIS is 0.4402 seconds, while for ANN, it is 0.5816 seconds. The maximum overshoot for ANFIS is 38.9241%, compared to 46.7343% for ANN. The ANFIS controller demonstrates superior recovery time, restoring functionality 1.2082 seconds after the disturbance is cleared.



**Fig. 15 Voltage and Current Response of ANN and ANFIS controller to Single line to ground fault at inverter end**

The response of both controllers to a single line-to-ground fault on phase A of the load side, simulated between 0.6 seconds and 0.7 seconds, is observed. The waveforms show that the ANN controller exhibits more oscillations, higher overshoot, and a longer time to reach steady state compared to the ANFIS controller. The ANFIS controller has better recovery time, restoring functionality 1.2536 seconds after the disturbance is cleared.



**Fig. 16 Active Power Response of ANN and ANFIS Controller to line-to-ground fault**  
 UGC CARE Group-1

The active power response to a single line-to-ground fault in an HVDC system is illustrated in Figure 16. The waveforms show a significant improvement in the performance of the ANFIS controller, with a steady state free of oscillations.

**TWO PHASE FAULT :**

A two-phase fault is induced on phases A and B of the load side at the inverter terminal to assess the operation of the rectifier and inverter. The fault occurs at 0.6 seconds and is cleared at 0.7 seconds. Figures 17, 18, and 19 illustrate the current, voltage, and power waveforms during the two-phase fault.

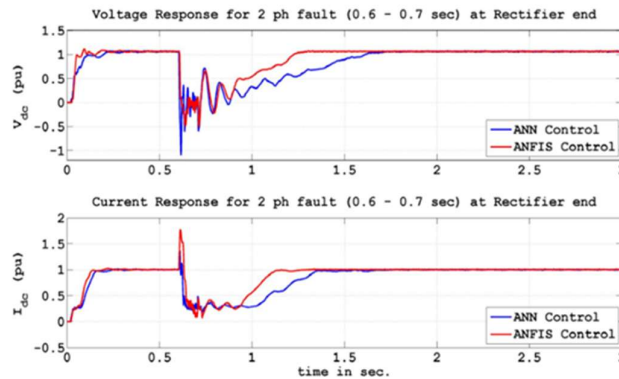


**Fig. 17 Voltage and Current Response of ANN and ANFIS controller to Two Phase fault at rectifier end**  
 The voltage and current waveforms are shown in Figure 17. The ANFIS controller reaches steady-state stability more quickly, with no overshoots, unlike the ANN controller. This highlights the resilience of the ANFIS controller, which restores functionality 1.2401 seconds after a two-phase failure is cleared.

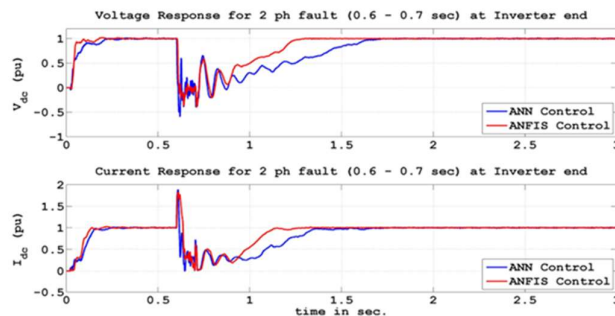


**Fig. 18 Voltage and Current Response of ANN and ANFIS controller to Two Phase fault at inverter end**

Phases A and B undergo a phase-phase evaluation from 0.6 seconds to 0.7 seconds. The waveforms are shown in Figure 18. The ANFIS controller shows significant improvement, with reduced transient oscillations and a faster response to steady state. In contrast, the ANN controller experiences slight oscillations around the final steady-state point, while the ANFIS controller maintains a steady state without any fluctuations.

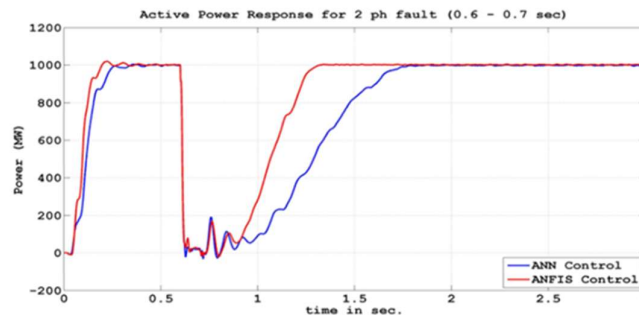


**Fig. 19 Active Power Response of ANN and ANFIS Controller to Two phase fault**

The ANFIS controller demonstrates a slight enhancement in active power relative to the standard ANN controller, as illustrated in Fig. 19. The Active power waveform indicates that DC power attains 1000MW within 1.2 seconds post-fault clearance.

### THREE PHASE FAULT :

A three-phase fault is assessed on phases A, B, and C of the load side at the inverter terminal to evaluate the performance of the rectifier and inverter. The fault occurs at 0.6 seconds and is cleared at 0.7 seconds. Figures 20, 21, and 22 illustrate the current, voltage, and power waveforms during the three-phase fault.

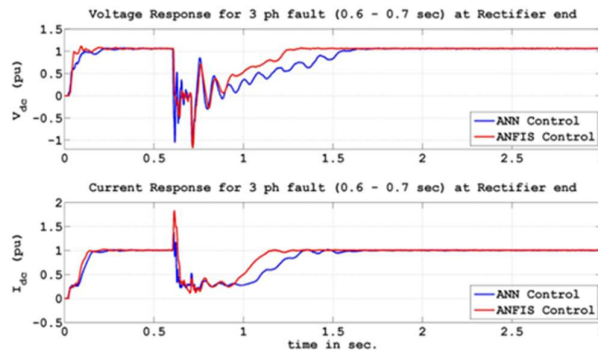


**Fig. 20 Response of ANN and ANFIS controller to Three Phase fault at rectifier end**

At 0.5 seconds, after the system reaches steady state following the dissipation of initial transients, a three-phase fault is initiated at the inverter end at 0.6 seconds and cleared at 0.7 seconds. Figure 20 illustrates the current and voltage waveforms. The current waveform shows that the ANFIS controller recovers more quickly than the ANN controller, with significantly reduced overshoot, fewer oscillations, and a smoother transition to steady state. The steady-state value is reached in 1.2534 seconds after the fault is cleared. The performance was analyzed for a three-phase fault occurring between 0.6 seconds and 0.7 seconds on the inverter load side.

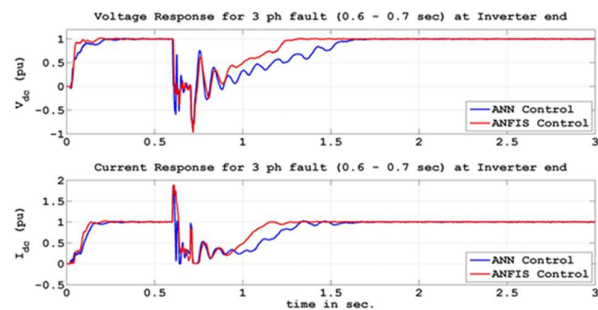


**Fig. 21 Response of ANN and ANFIS controller to Two Phase fault at inverter end**

Figure 21 illustrates the voltage and current waveforms. The voltage and current responses show that the ANFIS controller significantly improves performance over the ANN, with better oscillation damping, faster steady-state achievement, and a steady state free of oscillations. The steady-state value is reached in 1.2387 seconds after the fault is cleared.

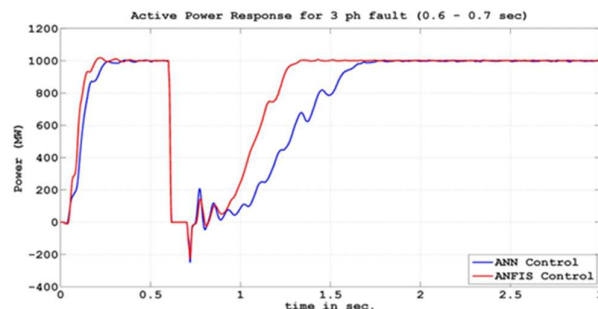


**Fig. 22 Active Power Response of ANN and ANFIS Controller to Three phase fault**

The active power waveform shown in Figure 22 illustrates that the ANFIS controller reduces oscillations and reaches steady state more smoothly than the ANN controller.

The performance parameters are summarized in Table 4 (Rectifier) and Table 5 (Inverter).

**Table 4 Rectifier performance characteristics with Artificial Neural Network (ANN) and ANFIS Controller**

	Rise Time (Sec.)		Settling Time (Sec.)		% Peak overshoot	
	ANN	ANFIS	ANN	ANFIS	ANN	ANFIS
DC Fault	0.1945	0.1462	1.4315	1.1585	60.7134	52.1127
S-L-G Fault	0.5816	0.4402	1.4805	1.2082	46.7343	38.9241
L-L Fault	0.6683	0.2381	1.6558	1.2401	57.3368	40.6882
Three Phase Fault	0.6053	0.4145	1.6479	1.2534	60.1016	42.3951

**Table 5 Inverter performance characteristics with Artificial Neural Network (ANN) and ANFIS Controller**

	Rise Time (Sec.)		Settling Time (Sec.)		% Peak over shoot	
	ANN	ANFIS	ANN	ANFIS	ANN	ANFIS
DC Fault	0.6897	0.4697	1.4473	1.1937	1.6017	1.2046
S-L-G Fault	0.7972	0.5266	1.5294	1.2536	1.4747	1.3023
L-L Fault	0.9394	0.5501	1.6881	1.2498	1.4392	1.2414
Three Phase Fault	0.7946	0.5656	1.6032	1.2387	1.4582	1.3431

The data in tables 4 and 5 indicate that both controllers enhance the performance of the HVDC system. When comparing rise time, settling time, peak, and percentage peak overshoot, the ANFIS demonstrates superior performance relative to ANN, Fuzzy, and PI controllers.

**CONCLUSION:**

This thesis addresses the improvement of power transfer capacity in a high-voltage direct current (HVDC) transmission system. The study described the implementation of an efficient and sophisticated current controller, developed using artificial intelligence techniques such as fuzzy logic, neural networks, and neuro-fuzzy logic, to enhance the gain in an HVDC transmission system. The HVDC transmission link was modeled utilizing MATLAB/SIMULINK with a 12-pulse thyristor converter. The CIGRE bench model 2 was employed in all studies conducted in this study endeavor.

The gain of the PI controller in an HVDC transmission system can be adaptively regulated utilizing fuzzy control, neural networks, and neuro-fuzzy systems to enhance performance. This dissertation presents several significant contributions. The principal contributions are delineated below.

A three-tier fuzzy logic controller was designed to regulate the gain of the standard PI controller. The system's performance enhanced with the implementation of a fuzzy logic controller. The oscillations noted after the disturbance with traditional PI control were significantly mitigated when a fuzzy logic controller was implemented. This applied to DC problems as well as various forms of AC faults. The system required roughly 1.80 seconds to attain a steady state.

An Artificial Neural Network (ANN) controller was designed to regulate the gain of the traditional PI controller. The system's performance enhanced with the implementation of an Artificial Neural Network (ANN) controller. The oscillations noted after the disturbance were substantially mitigated when employing an Artificial Neural Network (ANN) controller instead of conventional PI. This applied to DC problems as well as various forms of AC faults. The system required roughly 1.43 seconds to attain steady state.

An ANFIS controller was proposed to regulate the gain of the traditional PI controller. The system performance enhanced with the implementation of the ANFIS controller. The oscillations noted after the disturbance with the standard PI controller were significantly mitigated when the ANFIS controller



was employed. This applied to DC problems as well as various forms of AC faults. The system required around 1.15 seconds to attain a steady state.

In conclusion, it can be asserted that adaptively adjusting the gains of a standard PI controller with AI approaches significantly enhances the performance of the HVDC system.

#### REFERENCES:

- [1] J. Hou, G. Song, and Y. Fan, "Fault identification scheme for protection and adaptive reclosing in a hybrid multi-terminal HVDC system," *Prot. Control Mod. Power Syst.*, vol. 8, no. 1, pp. 1–17, 2023.
- [2] Y. Lin, Y. Tang, W. Wu, C. Ding, C. Zheng, and Y. Tang, "Cooperative reactive power configuration of hybrid HVDC transmission system for offshore wind farm clusters," in *2023 IEEE 7th Conference on Energy Internet and Energy System Integration (EI2)*, 2023, pp. 1161–1167.
- [3] S. S. Biswal, D. R. Swain, S. R. Paital, and P. K. Rout, "Voltage Stability Analysis of a Multi-Infed VSC based HVDC Transmission System," in *2023 IEEE 3rd International Conference on Sustainable Energy and Future Electric Transportation (SEFET)*, 2023, pp. 1–6.
- [4] G. Anwar, G. Ahmed, and C. Ali, "Stability analysis of voltage source converter control based HVDC system," in *2022 International Conference of Advanced Technology in Electronic and Electrical Engineering (ICATEEE)*, 2022, pp. 1–6.
- [5] B. Zhang, X. Du, C. Du, J. Zhao, and F. Li, "Stability modeling of a three-terminal MMC-HVDC transmission system," *IEEE Trans. Power Deliv.*, vol. 37, no. 3, pp. 1754–1763, 2022.
- [6] S. Wang, L. Zhou, T. Wang, T. Chen, and Y. Wang, "Fast protection strategy for DC transmission lines of MMC-based MT-HVDC grid," *Chin. J. Electr. Eng.*, vol. 7, no. 2, pp. 83–92, 2021.
- [7] T. Xu, S. Lin, D. Mu, and L. Zhao, "A novel fault area identification scheme for inverter station of HVDC based on wavelet energy ratio," in *2021 IEEE 5th Conference on Energy Internet and Energy System Integration (EI2)*, 2021, pp. 868–873.
- [8] X. Yu and L. Xiao, "A DC fault protection scheme for MMC-HVDC grids using new directional criterion," *IEEE Trans. Power Deliv.*, vol. 36, no. 1, pp. 441–451, 2021.
- [9] A. K. Tamrakar and E. Koley, "A SVM based fault detection and section identification scheme for a hybrid AC/HVDC transmission line with wind farm integration," in *2020 IEEE First International Conference on Smart Technologies for Power, Energy and Control (STPEC)*, 2020, pp. 1–5.
- [10] Y. Liang and Y. Huo, "A novel similarity-comparison-based directional protection scheme for multi-terminal HVDC grid," in *2020 IEEE 4th Conference on Energy Internet and Energy System Integration (EI2)*, 2020, pp. 3981–3986.
- [11] Arun and K. N. Chandra Bose, "Synchronverter based HVDC transmission for stability improvement," in *2019 International Conference on Intelligent Computing and Control Systems (ICCS)*, 2019, pp. 1312–1316.
- [12] I. Nassar, I. Elsayed, and M. Abdella, "Optimization and stability analysis of offshore hybrid renewable energy systems," in *2019 21st International Middle East Power Systems Conference (MEPCON)*, 2019, pp. 583–588.
- [13] A. Musa, A. Kaushal, S. K. Gurumurthy, D. Raisz, F. Ponci, and A. Monti, "Development and stability analysis of LSD-based virtual synchronous generator for HVDC systems," in *IECON 2018 - 44th Annual Conference of the IEEE Industrial Electronics Society*, 2018, pp. 3535–3542.
- [14] T. Bandaru, U. Dhawa, D. Chatterjee, and T. Bhattacharya, "Improving the transient stability by modifying the power exchange by the HVDC transmission," in *2018 20th National Power Systems Conference (NPSC)*, 2018, pp. 1–6.
- [15] T. Johnson and K. N. Shubhanga, "Response-type modelling of a two-terminal HVDC link for power system stability analysis," in *2017 Innovations in Power and Advanced Computing Technologies (i-PACT)*, 2017, pp. 1–6.